iScience

CellPress

Article

Glucose-Induced Cyclic Lipopeptides Resistance in Bacteria via ATP Maintenance through Enhanced Glycolysis

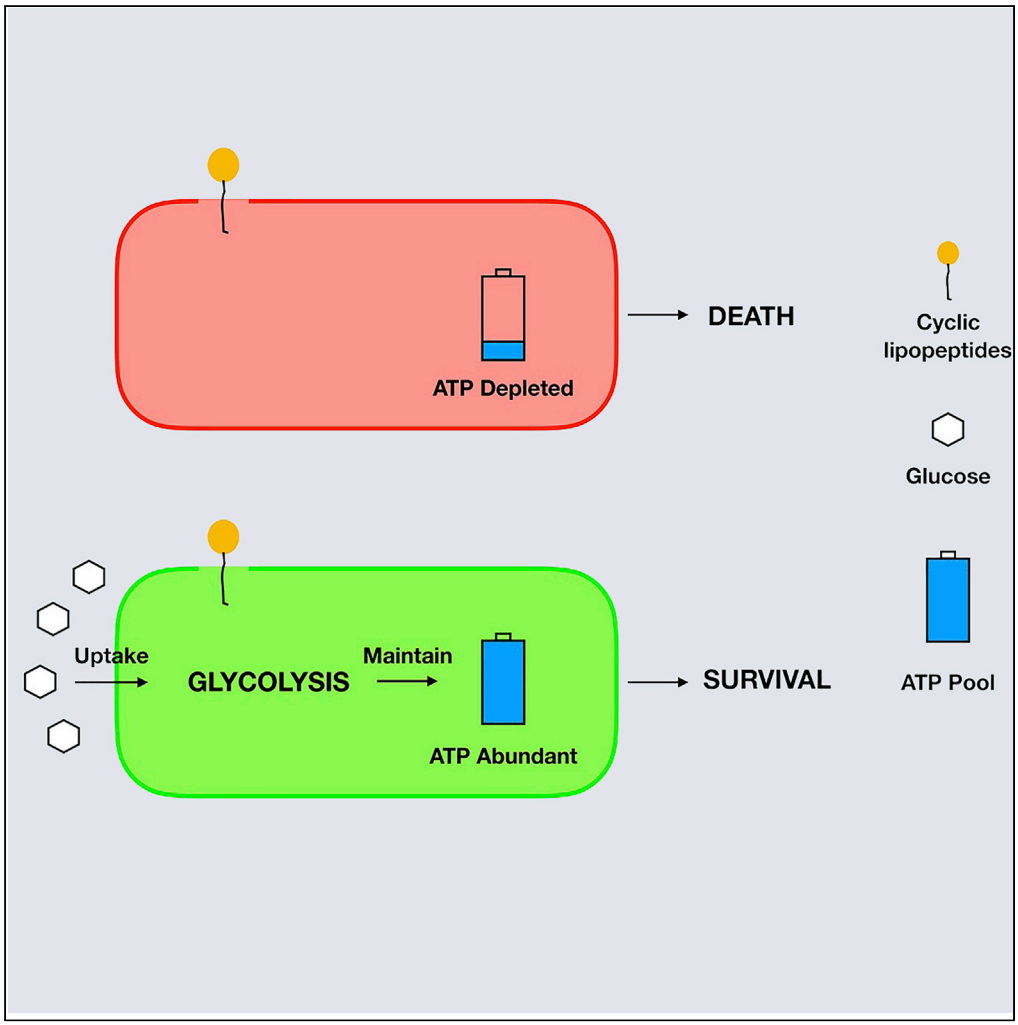

Wen-Bang Yu, Qian Pan, Bang-Ce Ye

bcye@ecust.edu.cn

HIGHLIGHTS

Glucose induces the drug resistance to CLPs

CLPs significantly inhibit energy metabolism and result in ATP depletion

Glucose maintains the intracellular ATP level in CLP-treated bacteria

Yu et al., iScience *21*, 135–144
November 22, 2019
https://doi.org/10.1016/j.isci.2019.10.009

iScience

CellPress

Article

Glucose-Induced Cyclic Lipopeptides Resistance in Bacteria via ATP Maintenance through Enhanced Glycolysis

Wen-Bang Yu,[1,2,4] Qian Pan,[1,4] and Bang-Ce Ye[1,3,5,*]

SUMMARY

Cyclic lipopeptide (CLP) antibiotics have a mechanism that causes membrane malfunction. Thus mechanisms of bacterial resistance to CLPs are thought to modify cell surfaces. However, we found that bacterial resistance to CLPs was strongly related to energy metabolism. Using polymyxin B (PB) as a model of CLPs, we showed that PB causes malfunction of respiration and serious depletion of ATP, contributing to PB-induced cell death and carbon starvation. Glucose addition could maintain the intracellular ATP level and reverse the carbon starvation response resulting from PB treatment. Another study revealed that glycolysis was stimulated by the presence of PB and glucose. The mechanism underlying glucose-enabled CLPs' resistance suggests that glucose could maintain the ATP level in PB-treated bacteria by enhancing glycolysis. Similar results were observed in *Staphylococcus aureus*, where daptomycin resistance was enhanced by glucose. These findings provide insight into the mode of action of CLPs and resistance to these antibiotics.

INTRODUCTION

Antibiotics are useful for treating bacterial infections. However, the worldwide emergence of drug-resistant bacteria is a great threat to antibiotic efficacy. Cyclic lipopeptides (CLPs) produced by diverse groups of bacteria are receiving more and more attention because of their broad-spectrum activity against microorganisms, including multidrug-resistant pathogens (Baltz, 2009; Straus and Hancock, 2006). All CLPs are composed of a circular oligopeptide linked to a fatty acid chain. They also have a similar mode of action, which involves membrane integrity impairment and dissipation of membrane potential (Straus and Hancock, 2006). In recent years, studies have revealed that CLPs might have a second mode of action (Baltz, 2009; Hamamoto et al., 2015; Trimble et al., 2016; Xing et al., 2014). A recently identified CLP, lysocin E, was shown to inhibit respiration in *Staphylococcus aureus* by directly interacting with menaquinone (Hamamoto et al., 2015). The well-studied daptomycin (DAP) could cause dissipation of membrane potential and cell death without damaging membrane integrity. Moreover, polymyxin B (PB) was found to inhibit NADH dehydrogenase (NDH) from the gram-positive bacterium *M. smegmatis* (Mogi et al., 2009).

DAP and PB are two important CLPs that have been used in medical treatment for decades. Unfortunately, pathogens resistant to DAP and PB have emerged (Miller et al., 2016). However, knowledge of the CLPs' resistance mechanism is restricted to the modification of the cell wall, cell membrane, or outer membrane (Bayer et al., 2013; Fischer et al., 2011; Wosten et al., 2000). The *dlt* operon in *S. aureus* could reduce the negative charge of the cell surface and keep DAP away from the cell membrane (Bayer et al., 2013). MprF is a DAP-resistant protein responsible for lysinylation of PG, which also reduces the negative charge of the cell surface in *S. aureus* (Bayer et al., 2013). Fischer et al. compared the transcriptomic and proteomic profiles of a DAP-resistant methicillin-resistant *S. aureus* strain with those of the DAP-sensitive strain (Fischer et al., 2011). Their results showed that many genes involved in cell wall metabolism were significantly up-regulated in the DAP-resistant isolate, indicating the important role of cell wall in DAP resistance (Fischer et al., 2011). PmrA-PmrB in *Salmonella* is a two-component system that responds to the cellular iron level, induces the expression of genes involved in outer membrane modification, and confers PB resistance (Wosten et al., 2000).

Glucose is a prior carbon source that can support rapid growth of microorganisms (Sonenshein, 2007). Several recent studies showed that glucose and other carbon sources such as mannitol, fructose, and glycerol could affect the antibiotic sensitivity of the microorganism by regulating the metabolic state. Allison et al. found that these carbon sources could activate the membrane potential of *Escherichia coli* persisters,

[1]Laboratory of Biosystems and Microanalysis, State Key Laboratory of Bioreactor Engineering, East China University of Science and Technology, Shanghai 200237, China

[2]Jinhua Polytechnic, Jinhua, Zhejiang 321007, China

[3]Institute of Engineering Biology and Health, Collaborative Innovation Center of Yangtze River Delta Region Green Pharmaceuticals, College of Pharmaceutical Sciences, Zhejiang University of Technology, Hangzhou, Zhejiang 310014, China

[4]These authors contributed equally

[5]Lead Contact

*Correspondence: bcye@ecust.edu.cn

https://doi.org/10.1016/j.isci.2019.10.009

thus potentiating their sensitivity to aminoglycosides (Allison et al., 2011). Similarly, Peng et al. showed that glucose could restore antibiotic-resistant bacterial sensitivity to antibiotics by increasing the proton motive force (PMF), which mediates the uptake of antibiotics (Peng et al., 2015). Here, we found that glucose and some carbon sources exert an effect on bacterial resistance to CLPs and reveal a distinct mechanism underlying interaction between the metabolic state of bacteria and the bactericidal activity of antibiotics. PB caused respiratory malfunction and serious depletion of ATP, contributing to PB-induced cell death and an obvious carbon starvation response. The addition of glucose could maintain the intracellular ATP level and reverse the carbon starvation response resulting from treatment of PB. The results indicated that glucose induced bacterial resistance to PB by maintaining the intracellular ATP level in PB-treated bacteria through enhanced glycolysis. Similar results were also observed in *S. aureus*, where DAP resistance was enhanced by glucose. These findings demonstrated that the intracellular ATP level was important for the mode of action of CLPs, and they provide insight into bacterial resistance to these antibiotics.

RESULTS

Glucose-Induced Drug Resistance to CLPs

We previously studied the mode of action of CLPs on *B. subtilis* using transcriptome analysis, which revealed that CLPs caused significant carbon starvation (Yu et al., 2012). We wondered if the bactericidal activity of CLPs was related to carbon metabolism. Here, we investigated the effect of some carbon sources (20 mM glucose, fructose, glycerol, and arabinose) on the bactericidal activity of PB in *B. subtilis* (Figures 1A and B). *B. subtilis* cells incubated in Luria broth medium with or without carbon sources were treated with 50 μg/mL PB. As shown in Figures 1A and 1B, both glucose and fructose significantly enhanced drug resistance to PB in *B. subtilis*. Glycerol and arabinose had weaker effect on PB resistance in *B. subtilis* (Figure 1B). To study if glucose-induced resistance is applicable to other CLPs, we tested the effect of glucose on *B. subtilis*' resistance to DAP. As shown in Figure 1C, glucose also enhanced *B. subtilis*' resistance to DAP. With increase in glucose concentrations, bacterial resistance to DAP increased. However, these results showed that higher concentration of glucose (15 mM) was needed to completely inhibit the activity of DAP with a concentration of 5 μg/mL (Figure 1C). This might be because the activity of DAP is more efficient than that of PB when treating *B. subtilis*. We also tested if glucose induced resistance to other cationic antimicrobial peptides (such as vancomycin [VAN]). However, with the presence of glucose, resistance of *B. subtilis* to VAN was not enhanced (Figure 1D).

To investigate the relationship between carbon metabolism and the action of CLPs, proteomic analysis was performed with *B. subtilis* cells treated with PB, PB plus glucose, or glucose. After applying a cutoff value of 1.2-fold change ($p < 0.05$), the expressions of 805, 594, and 478 proteins were found to be significantly changed after treatment by PB, PB plus glucose, or glucose, respectively (Figure S1 and Table S1). As shown in the Figure 2, MalP and ManP were involved in mannose uptake, MtlA was involved in mannitol uptake, LevDE was involved in fructose uptake, GlpTK was involved in glycerol uptake, AcoL was involved in acetoin catabolism, RocG was involved in glutamate catabolism and the proteins SdhAB that compose the succinate dehydrogenase complex, AcsA was involved in acetate utilization, and GapB was involved in glucogenesis, and they were all significantly up-regulated in PB-treated *B. subtilis* (Figure 2). However, no change was observed in *B. subtilis* treated with PB plus glucose (Figure 2). Pgi, Pgk, Eno, FbaA, and Ldh were involved in the glycolysis pathway, and they were significantly down-regulated by PB treatment. None of them were down-regulated after treatment with PB plus glucose. In *B. subtilis*, alternative carbon acquisition or metabolism is repressed, whereas catabolism of glucose is activated by CcpA, which senses the energy status of the cell and is activated by fructose-1,6-bisphosphate (FBP) or high ATP concentrations (Ludwig et al., 2001; Sonenshein, 2007). These results might indicate that PB resulted in a lower energy status before being reverted by glucose.

The proteins involved in respiration are also shown in Figure 2. PB repressed cytochrome caa3 (CtaCDF), menaquinol-cytochrome c reductase (QcrABC), and cytochrome bd (CydA) expression, but it induced NADH-Q dehydrogenase (YjlD, renamed Ndh) and succinate dehydrogenase (SdhAB) expression. It seems that PB led to respiratory malfunction. Mogi et al. reported that PB can inhibit NADH-Q dehydrogenase in *M. smegmatis* (Mogi et al., 2009). It is possible that PB could inhibit NADH-Q dehydrogenase, causing $NADH/NAD^+$ and Q/QH_2 increases that lead to Ndh induction and repression of CtaCDF, QcrABC, and CydA. In *B. subtilis*, Ndh expression is induced by an increased $NADH/NAD^+$ ratio (Gyan et al., 2006), whereas CydA, QcrABC, and CtaCDF expression might be repressed due to an increased Q/QH_2 ratio (Geng et al., 2007). After PB plus glucose treatment, expression of QcrABC and CtaCDF was also

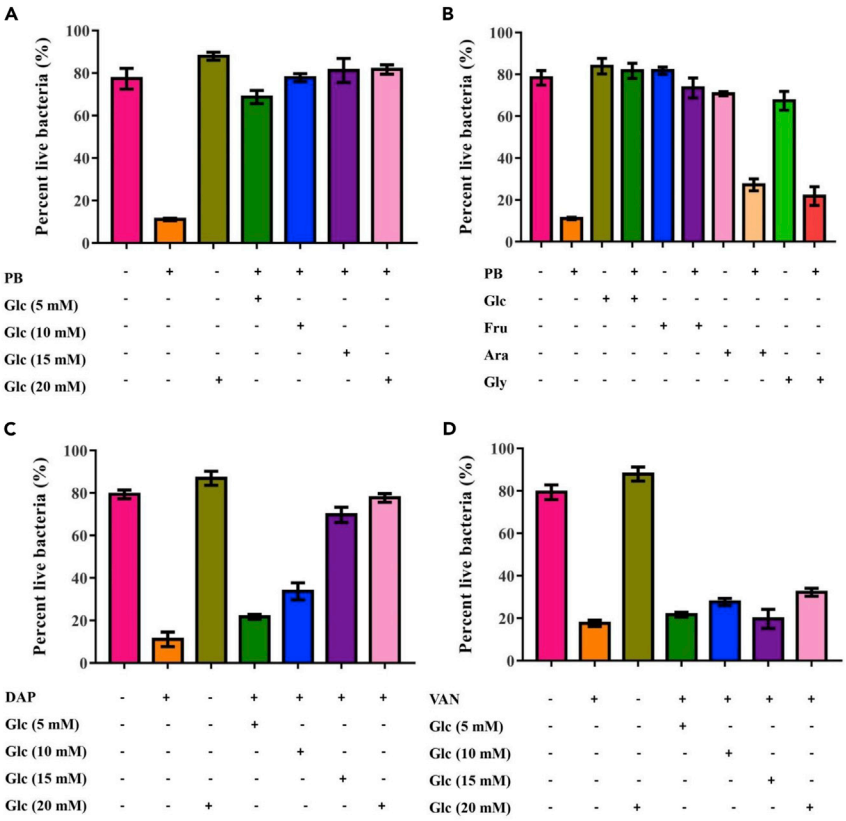

Figure 1. Glucose-Induced Drug Resistance to CLPs

Three biological replicates were used for each assay. Data are represented as mean ± SD.

(A) Live percentage of *B. subtilis* culture after no treatment (control) and treatment of PB, glucose (Glc), and PB plus 5, 10, 15, and 20 mM Glc.

(B) Live percentage of *B. subtilis* culture after no treatment and treatment of PB, Glc, PB plus Glc, fructose (Fru), PB plus Fru, arabinose (Ara), PB plus Ara, glycerol (Gly), and PB plus Gly. The pyruvate cycle increases aminoglycosides' efficacy and provides respiratory energy in bacteria.

(C) Live percentage of *B. subtilis* culture after no treatment and treatment of DAP, Glc, and DAP plus 5, 10, 15, and 20 mM Glc.

(D) Live percentage of *B. subtilis* culture after no treatment, VAN, Glc, and VAN plus 5, 10, 15, and 20 mM Glc.

significantly repressed. However, Ndh expression was less up-regulated, and CydA was significantly up-regulated. These observations indicated that glucose could revert the NADH/NAD^+ increase and cause some degree of respiratory malfunction.

PB Inhibited NADH Dehydrogenase and ATP Synthesis, Leading to ATP Depletion

The proteomics results revealed an increase in the NADH/NAD^+ ratio, and Mogi et al. reported that PB can inhibit NADH-Q dehydrogenase in *M. smegmatis*. We reasoned that PB might also inhibit respiratory NDH in *B. subtilis* (Mogi et al., 2009). To test this, *B. subtilis* cell membrane preparation was treated with or without PB in the presence of menaquinone and NADH. As shown in Figure 3, the decreasing velocity of NADH was much slower with PB, indicating that NDH enzyme activity was inhibited by PB (Figure 3A). The IC50 values of PB to NDH were determined to be 18.82 μg/mL. *B. subtilis* is a facultative anaerobe whose ATP was mainly supplied by aerobic respiration under aerobic conditions. Inhibition of respiratory NDH might inhibit ATP synthesis. Moreover, PB causes dissipation of PMF, which activates F0-F1 ATP synthetase (Maloney et al., 1974). This result suggested that PB might inhibit ATP synthesis *in vivo*. The intracellular ATP level in PB-treated bacteria was determined using the ATP-analyzing kit. We found that the ATP level decreased in PB-treated bacteria in a dose-dependent manner (Figure 3B). To examine if ATP depletion results in the bactericidal action of PB, *B. subtilis* was pretreated with 1 mM dicyclohexylcarbodiimide (DCCD), which is an inhibitor of F0-F1 ATP synthase. As shown in Figures 3C and 3D, *B. subtilis*

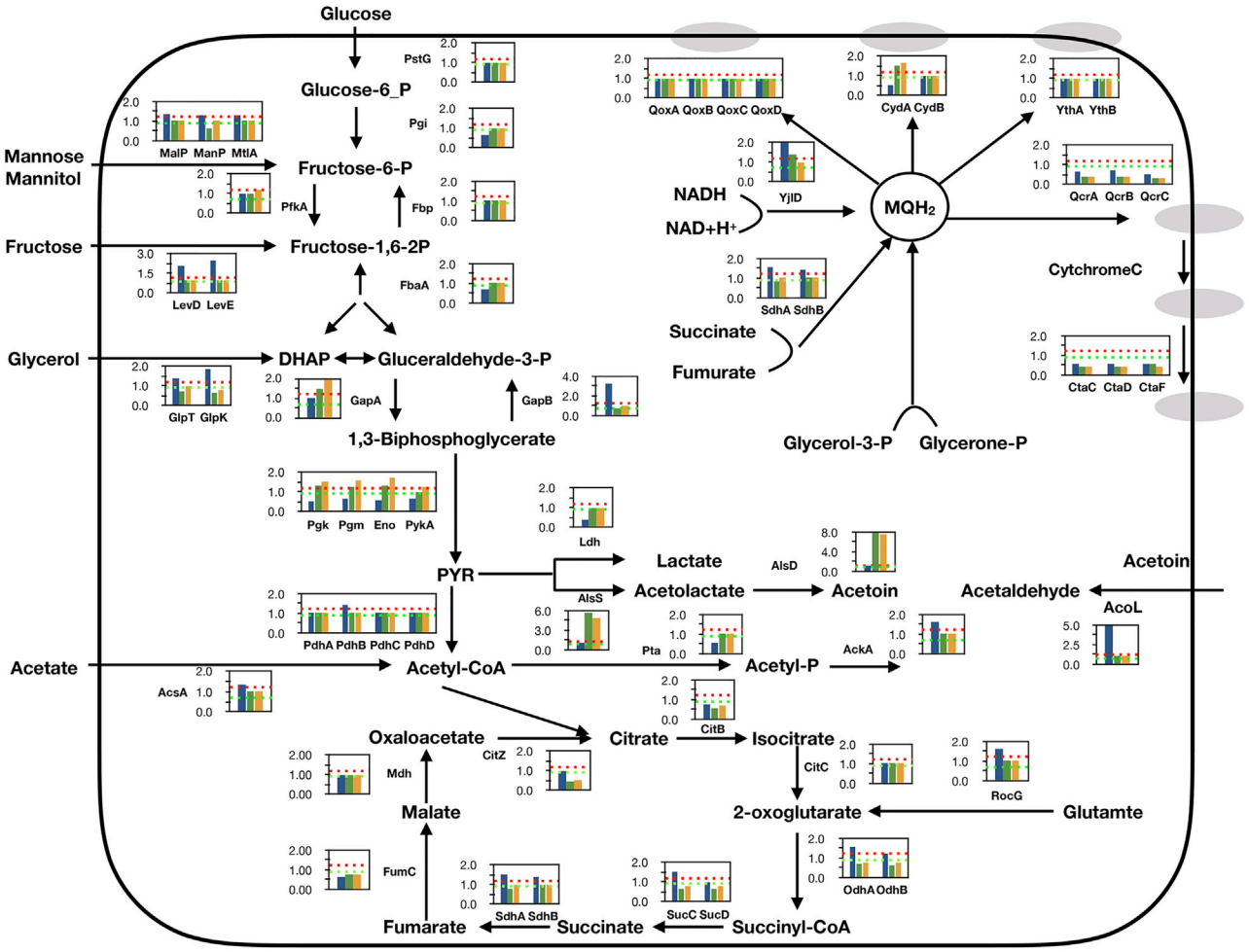

Figure 2. Expression Levels of Proteins Involved in Carbon Metabolism and Aerobic Respiration of *B. subtilis* Treated with PB, PB Plus Glucose, or Glucose

Three columns from left to right represent expression ratios of proteins in response to treatment of PB (blue), PB plus glucose (green), and glucose (yellow). Two dotted lines were used to indicate the cutoff value: red line (1.2-fold) and green line (0.83-fold).

pretreated with DCCD were more sensitive to PB, which is indicated by a faster OD600 drop and lower ATP level. These results indicated that PB caused ATP depletion and contributed to cell death.

Glucose Maintained the Intracellular ATP Level in PB-Treated *B. subtilis*

Glucose is a key carbon source that supplies energy for bacterial growth (Sonenshein, 2007). This could keep the intracellular ATP level in PB-treated bacteria. To test this, the intracellular ATP levels were analyzed in the presence of PB, PB plus glucose, or glucose. As shown in Figure 4, ATP levels in PB-treated bacteria were much lower than that in the control. However, this was reverted by glucose, which increased the ATP level in the PB-treated bacteria to about 2-fold compared with control (Figure 4). It was noted that the ATP level in the PB plus glucose treatment was much lower than in the glucose only treatment, indicating that PB still inhibited ATP synthesis even in the presence of glucose.

In bacteria, glucose can generate ATP via glycolysis or the electron transport chain (ETC). To investigate if glucose enhanced ATP synthesis via ETC after PB treatment, we examined the PMF of the *B. subtilis* treated with PB or PB plus glucose. As shown in Figure 5A, the PMF of PB-treated bacteria was increased to some degree by glucose, but that was still lower than the PMF of the untreated bacteria. Fructose that enabled drug resistance had no effect on the PMF in PB-treated bacteria (Figure 5A). As glucose did not restore the PMF to the control level, we suggested that glucose might stimulate glycolysis to generate ATP in the

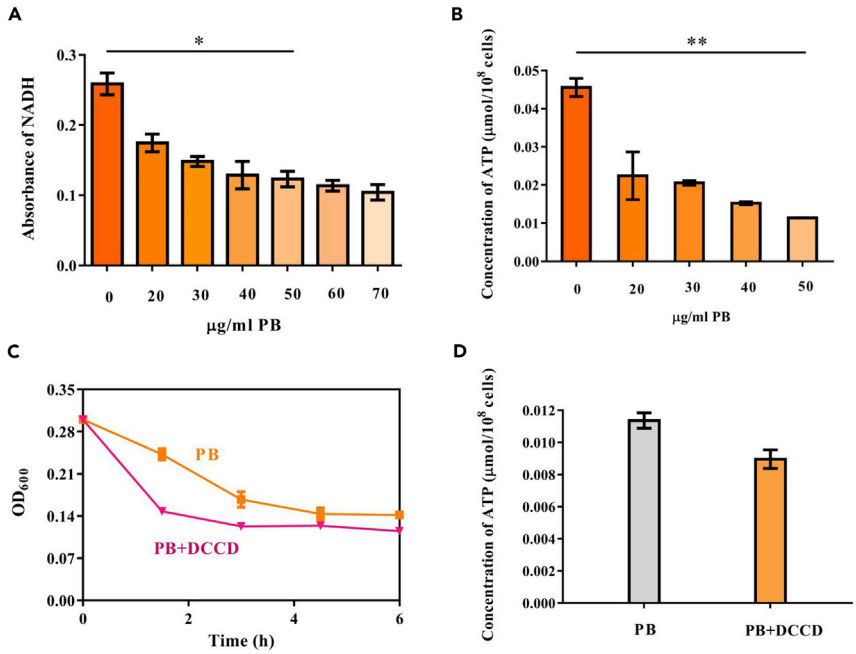

Figure 3. PB Inhibited NADH Dehydrogenase and ATP Synthesis

Three biological replicates were used for each assay. Data are represented as mean ± SD.

(A) Activity of membrane-bound NADH dehydrogenase after treatment of different concentrations of PB (20, 30, 40, 50, 60, 70 μg/mL). The absorbance level of NADH in the treatments of PB (0, 20, 30, 40, 50 μg/mL) was significantly different.

(B) *In vivo* ATP levels of *B. subtilis* after treatment of different concentrations of PB (20, 30, 40, 50 μg/mL). The concentration of ATP in each sample was significantly different.

(C) Growth curve of *B. subtilis* after treatment of PB and PB plus DCCD.

(D) *In vivo* ATP levels of *B. subtilis* after treatment of PB and PB plus DCCD. *$p < 0.05$, **$p < 0.01$ by one-way ANOVA t test.

presence of PB. To support this, we determined the intracellular metabolites (glucose, pyruvate, and acetate) of the glycolytic pathway to analyze glycolytic activity. As shown in Figures 5B–5D, the intracellular levels of these metabolites were significantly lower in the PB-treated *B. subtilis* than in the untreated ones, indicating that PB led to carbon source depletion and low glycolytic activity. However, the intracellular concentrations of glucose, pyruvate, and acetate were greatly increased in the PB treatment plus glucose, suggesting that glucose reverses carbon starvation and low glycolysis in the PB-treated bacteria. In the presence of PB, *B. subtilis* would uptake more glucose and increase the glycolytic pathway flux. These results showed that glucose induced bacterial resistance to PB by increasing intracellular ATP level via enhancement of glycolysis.

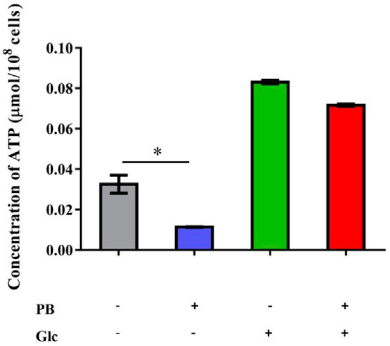

Figure 4. Determination of Intracellular ATP Levels of *B. subtilis* with No Treatment and Treatment of PB, Glucose (Glc), and PB Plus Glc

Data are represented as mean ± SD. The ATP concentrations of the samples with no treatment and treatment of PB were significantly different (*$p < 0.05$).

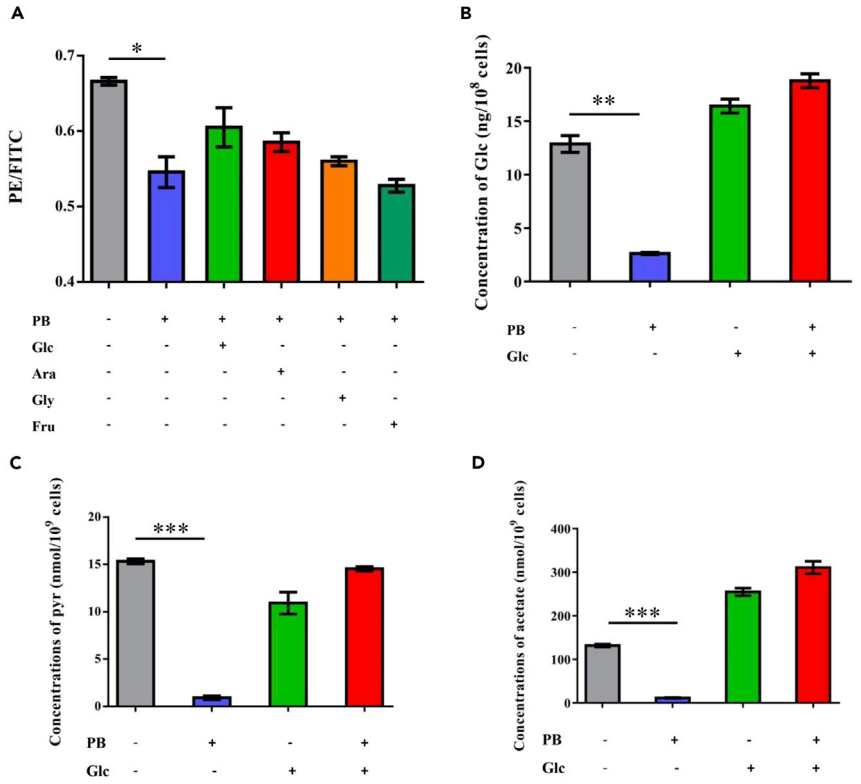

Figure 5. Analysis of PMF and Glycolysis Metabolites

Three biological replicates were used for each assay. Data are represented as mean ± SD.

(A) PMF of *B. subtilis* with no treatment and treatment of PB plus no metabolite (PB), glucose (PB + Glc), arabinose (PB + Ara), glycerol (PB + Gly), and fructose (PB + Fru). The PMF of the samples with no treatment and treatment of PB were significantly different.

(B) Intracellular glucose levels of *B. subtilis* with no treatment and treatment of PB, glucose (Glc), and PB plus glucose (PB + Glc). The glucose concentrations of the samples with no treatment and treatment of PB were significantly different.

(C) Intracellular levels of pyruvate (Pyr) of *B. subtilis* with no treatment and treatment of PB, glucose (Glc), and PB plus glucose (PB + Glc). The pyruvate concentrations of the samples with no treatment and treatment of PB were significantly different.

(D) Intracellular levels of acetate of *B. subtilis* with no treatment and treatment of PB, glucose (Glc), and PB plus glucose (PB + Glc). The acetate concentrations of the samples with no treatment and treatment of PB were significantly different.

*$p < 0.05$, **$p < 0.01$, ***$p < 0.001$ by one-way ANOVA t test.

Glycolysis Is the Key Pathway that Enables PB Resistance in *B. subtilis*

To confirm that glycolysis enables PB resistance, the bacteria were treated with cysteine, an inhibitor of pyruvate kinase, to inhibit glycolysis flux (Kedryna et al., 1983). As shown in Figure 6A, in the presence of cysteine, glucose could not induce resistance to PB in *B. subtilis*. We also tested the effect of the tricarboxylic acid (TCA) cycle on glucose-enabled drug resistance by treating *B. subtilis* with a high concentration of malonic acid (20 mM), an inhibitor of succinate dehydrogenase, to inhibit TCA flux (Lu et al., 2018) (Figure 6C). Malonic acid did not eliminate glucose-enabled drug resistance, but the live percentage of the PB plus glucose plus malonic acid treatment was slower than the PB plus glucose treatment. These observations demonstrated that glycolysis was essential in glucose-enabled drug resistance, but the TCA cycle was not essential. Glucose catabolism could generate NADH, which is oxidized by ETC, contributes to PMF, and activates F0-F1 ATP synthase to generate ATP. Next, we investigated the effect of F0-F1 ATP synthase on glucose-enabled resistance by treating *B. subtilis* with DCCD, an inhibitor of F0-F1 ATP synthase (Rao et al., 2008). With a DCCD supplement, we found that PB resistance could be eliminated by 2 mM DCCD. This result indicated that F0-F1 ATP synthase might also contribute to glucose-enabled drug resistance (Figure 6B).

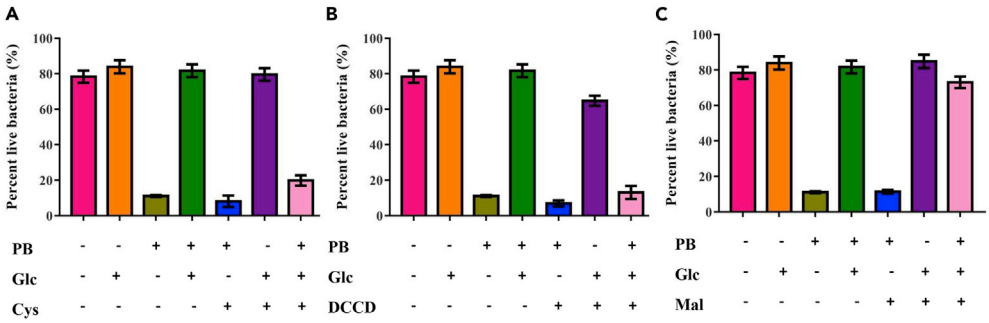

Figure 6. Effect of Inhibitors on Glucose-Induced Drug Resistance

Data are represented as Mean ± SD.

(A) Live percentage of *B. subtilis* after no treatment (Control) and treatment of Glc, PB, PB plus glucose (PB + Glc), PB plus cysteine (PB + Cys), glucose plus cysteine (Glc + Cys), and PB plus glucose plus cysteine (PB + Glc + Cys).

(B) Live percentage of *B. subtilis* after no treatment (Control) and treatment of Glc, PB, PB plus glucose (PB + Glc), PB plus DCCD (PB + DCCD), glucose plus DCCD (Glc + DCCD), and PB plus glucose plus DCCD (PB + Glc + DCCD).

(C) Live percentage of *B. subtilis* after no treatment (Control) and treatment of Glc, PB, PB plus glucose (PB + Glc), PB plus malonic acid (PB + Mal), glucose plus malonic acid (Glc + Mal), and PB plus glucose plus malonic acid (PB + Glc + Mal).

Glucose Also Induced Bacterial Resistance to CLPs in *Staphylococcus aureus*

After showing that glucose induces resistance to CLPs in *B. subtilis*, we investigated if the phenomenon is applicable to *S. aureus*. As *S. aureus* is not sensitive to PB, we treated *S. aureus* with DAP (5 μg/mL). The results showed that DAP also resulted in serious ATP depletion leading to cell death in *S. aureus* (Figures 7A and 7B). With the addition of glucose, the ATP level was maintained and the killing activity of DAP was inhibited (Figures 7A and 7B). Moreover, we observed that glucose-induced drug resistance to CLPs in *S. aureus* was eliminated by cysteine (Figure 7A). Collectively, these observations demonstrated that glucose induces bacterial resistance to CLPs in *S. aureus* through the same mechanism as it does in *B. subtilis*.

DISCUSSION

Previous knowledge about the mechanism of CLPs' resistance in bacteria was restricted to cell surface modifications. However, we found that glucose could enable bacterial resistance to CLPs. To understand how glucose enables bacterial resistance to CLPs, we re-investigated CLPs' action using PB as a model CLP. The CLPs' mechanism was supposed to destroy lipid bilayer membrane integrity and cause dissipation of membrane potential (Straus and Hancock, 2006). However, several studies showed that the destruction of membrane integrity was not the sole killing mechanism in the action of CLPs (Baltz, 2009; Hamamoto et al., 2015; Mogi et al., 2009; Trimble et al., 2016; Xing et al., 2014). That is because cellular processes such as cell division, cell wall component synthesis, and energetics are affected by membrane integrity (Baltz, 2009; Straus and Hancock, 2006). In a recent study by Mogi et al., PB was found to be a potent inhibitor of membrane-bound NDH from *M. smegmatis*, indicating that PB might disturb the energetic status (Mogi et al., 2009). Here, we investigated the energy status of PB-treated bacteria. We found that PB would cause significant ATP depletion in *B. subtilis*. This contributed to its killing action, indicating that energetics is a PB target. Furthermore, we found that glucose could maintain the intracellular ATP level in PB-treated bacteria. We suggested that glucose enables bacterial PB resistance by maintaining the ATP level.

To scrutinize how glucose maintains the ATP level in PB-treated bacteria, we used proteomic analysis to investigate the metabolic status of bacteria after PB treatment. The results revealed that PB inhibited membrane-bound NDH in *B. subtilis* and caused down-regulation of respiration complexes, indicating that PB caused respiratory malfunction. PB treatment also caused PMF dissipation. These were the reasons why PB caused ATP depletion. PB treatment caused a significant response of carbon starvation. First, many proteins involved in transport and catabolism of alternative carbon sources were up-regulated (Ludwig et al., 2001; Sonenshein, 2007). Second, PB treatment also caused significant decrease in the levels of carbon metabolites *in vivo*, including glucose, pyruvate, and acetate. Thus, this could be explained by the fact that PB leads to low energy status and so more carbon sources were catabolized to maintain the energy status for survival. As a result, *in vivo* carbon metabolites were exhausted. However, this carbon starvation state was reverted by glucose. With a supplement of glucose, the bacteria could achieve enough carbon

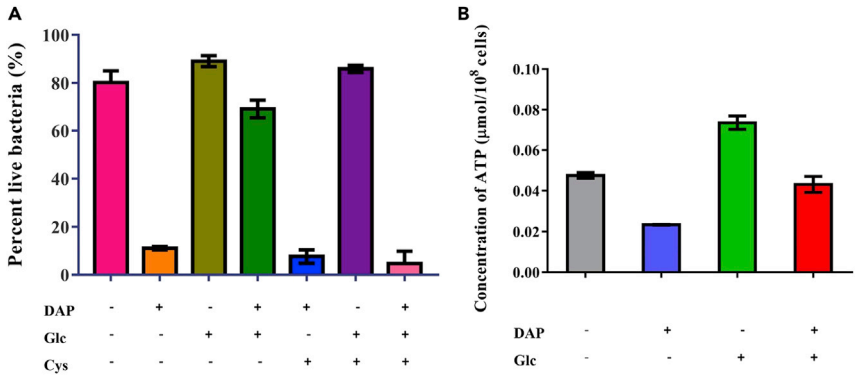

Figure 7. Glucose Induced *S. aureus*' Resistance to CLPs

Data are represented as mean ± SD.

(A) Live percentage of *S. aureus* after no treatment (Control) and treatment of DAP, Glc, DAP plus glucose (DAP + Glc), DAP plus cysteine (DAP + Cys), glucose plus cysteine (Glc + Cys), and DAP plus glucose plus cysteine (DAP + Glc + Cys).

(B) *In vivo* ATP levels of *S. aureus* after no treatment and treatment of DAP, glucose (Glc), and DAP plus glucose (DAP + Glc).

sources for survival. Owing to inhibition of respiration, the bacteria might maintain the energy status by enhancing glycolysis. To confirm this hypothesis, we compared the levels of the glycolytic metabolites, including glucose, pyruvate, and acetate in PB/glucose- and glucose-treated bacteria. The results showed that levels of the glucose, pyruvate, and acetate are much higher in PB/glucose-treated bacteria, demonstrating that glycolysis was enhanced by PB.

We also explored the role of the TCA cycle and F0-F1 ATP synthase in glucose-enabled drug resistance. The drug resistance could be eliminated by a high concentration of DCCD but not by malonic acid. This indicated that F0-F1 ATP synthase might partially contribute to PB resistance, but TCA does not. It seemed that glycolysis alone could not sustain survival of PB-treated bacteria in the glucose test concentration range. However, DCCD might have an additional effect, which causes dissipation of PMF in *B. subtilis* (Calamita et al., 2001). As glucose had no significant effect on restoration of the PMF, DCCD may cause a further dissipation of PMF, which may lead to cell lysis in *B. subtilis* (Calamita et al., 2001).

Inhibition of NDH will restrict NADH/NAD^+ turnover leading to NAD^+ limitation *in vivo* (Gyan et al., 2006). As NAD^+ is the main oxidant in the cell, restoration of the NAD^+ pool makes NADH turnover a top priority compared with ATP synthesis (Yang et al., 2018). As seen in the proteomic results, NDH expression was 2-fold up-regulated in PB treatment but 1.3-fold up-regulated in PB plus glucose treatment. This indicated that glucose might revert the increase in NADH/NAD^+. Here, we noted that NadA and NadB involved in NAD^+ synthesis were significantly up-regulated (2.2-fold and 3.2-fold, respectively) with glucose supplement, but these two proteins were down-regulated (0.51-fold and 0.60-fold, respectively) with PB treatment. Thus, it was possible that glucose increased the NAD^+ pool to revert the increase in NADH/NAD^+. However, this hypothesis needs to be further confirmed.

This work demonstrated that bacterial sensitivity to CLPs is strongly related to energy metabolism. The relation between bacterial resistance to antibiotics and energy metabolism is also observed elsewhere (Cheng et al., 2018; Liu et al., 2019; Su et al., 2018). Herein, we showed that CLPs could disturb ATP synthesis and cause cell death, but glucose can maintain the ATP level by enhancing glycolysis and enabling drug resistance (Figure 8). This study provides insight into the mode of action of CLPs and bacterial resistance mechanisms to CLPs.

Limitations of the Study

In this study, the molecular mechanism underlying ATP depletion induced by CLP antibiotics remains unclear.

METHODS

All methods can be found in the accompanying Transparent Methods supplemental file.

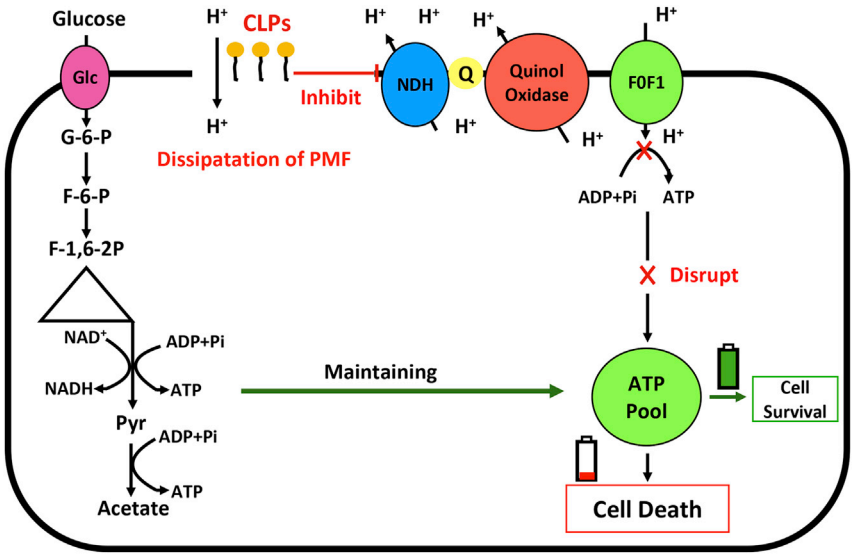

Figure 8. The Mechanism Underlying Glucose-Induced Bacterial Resistance to CLPs

CLPs inhibit aerobic respiration and cause PMF dissipation, leading to ATP depletion and contributing to cell death. Glucose maintains the ATP level by enhancing glycolysis and maintaining cell survival.

SUPPLEMENTAL INFORMATION

Supplemental Information can be found online at https://doi.org/10.1016/j.isci.2019.10.009.

ACKNOWLEDGMENTS

This study was supported by grants from the National Natural Science Foundation of China (31730004) and the National Key Research and Development Program of China (2018YFA0900404).

AUTHOR CONTRIBUTIONS

Conceptualization, W.-B.Y., Q.P., and B.-C.Y.; Methodology, Q.P.; Resources, B.-C.Y.; Formal Analysis, W.-B.Y. and Q.P.; Writing – Original Draft, W.-B.Y.; Writing – Review & Editing, W.-B.Y., Q.P., and B.-C.Y.; Supervision, B.-C.Y.; Funding Acquisition, B.-C.Y.

DECLARATION OF INTERESTS

The authors declare no competing interests.

Received: March 1, 2019
Revised: June 20, 2019
Accepted: October 1, 2019
Published: November 22, 2019

REFERENCES

Allison, K.R., Brynildsen, M.P., and Collins, J.J. (2011). Metabolite-enabled eradication of bacterial persisters by aminoglycosides. Nature *473*, 216–220.

Baltz, R.H. (2009). Daptomycin: mechanisms of action and resistance, and biosynthetic engineering. Curr. Opin. Chem. Biol. *13*, 144–151.

Bayer, A.S., Schneider, T., and Sahl, H.G. (2013). Mechanisms of daptomycin resistance in *Staphylococcus aureus*: role of the cell membrane and cell wall. Ann. N. Y Acad. Sci. *1277*, 139–158.

Calamita, H.G., Ehringer, W.D., Koch, A.L., and Doyle, R.J. (2001). Evidence that the cell wall of *Bacillus subtilis* is protonated during respiration. Proc. Natl. Acad. Sci. U S A *98*, 15260–15263.

Cheng, Z.X., Yang, M.J., Peng, B., Peng, X.X., Lin, X.M., and Li, H. (2018). The depressed central carbon and energy metabolisms is associated to the acquisition of levofloxacin resistance in *Vibrio alginolyticus*. J. Proteomics *181*, 83–91.

Fischer, A., Yang, S.J., Bayer, A.S., Vaezzadeh, A.R., Herzig, S., Stenz, L., Girard, M., Sakoulas, G., Scherl, A., Yeaman, M.R., et al. (2011). Daptomycin resistance mechanisms in clinically derived *Staphylococcus aureus* strains assessed by a combined transcriptomics and proteomics approach. J. Antimicrob. Chemother. *66*, 1696–1711.

Geng, H., Zuber, P., and Nakano, M.M. (2007). Regulation of respiratory genes by ResD-ResE signal transduction system in *Bacillus subtilis*. Methods Enzymol. *422*, 448–464.

Gyan, S., Shiohira, Y., Sato, I., Takeuchi, M., and Sato, T. (2006). Regulatory loop between redox sensing of the NADH/NAD(+) ratio by Rex (YdiH)

and oxidation of NADH by NADH dehydrogenase Ndh in *Bacillus subtilis*. J. Bacteriol. *188*, 7062–7071.

Hamamoto, H., Urai, M., Ishii, K., Yasukawa, J., Paudel, A., Murai, M., Kaji, T., Kuranaga, T., Hamase, K., Katsu, T., et al. (2015). Lysocin E is a new antibiotic that targets menaquinone in the bacterial membrane. Nat. Chem. Biol. *11*, 127–U168.

Kedryna, T., Guminska, M., and Marchut, E. (1983). The inhibitory effect of L-cysteine and its derivatives on glycolysis in Ehrlich ascites tumour cells. Biochim. Biophys. Acta *763*, 64–71.

Liu, S.R., Peng, X.X., and Li, H. (2019). Metabolic mechanism of ceftazidime resistance in *Vibrio alginolyticus*. Infect. Drug Resist. *12*, 417–429.

Lu, Q., Zhao, Y., Gao, X.T., Wu, J.Q., Zhou, H.X., Tang, P.F., Wei, Q.B., and Wei, Z.M. (2018). Effect of tricarboxylic acid cycle regulator on carbon retention and organic component transformation during food waste composting. Bioresour. Technol. *256*, 128–136.

Ludwig, H., Homuth, G., Schmalisch, M., Dyka, F.M., Hecker, M., and Stulke, J. (2001). Transcription of glycolytic genes and operons in *Bacillus subtilis*: evidence for the presence of multiple levels of control of the gapA operon. Mol. Microbiol. *41*, 409–422.

Maloney, P.C., Kashket, E.R., and Wilson, T.H. (1974). A proton motive force drives ATP synthesis in bacteria. Proc. Natl. Acad. Sci. U S A *71*, 3896–3900.

Miller, W.R., Bayer, A.S., and Arias, C.A. (2016). Mechanism of action and resistance to daptomycin in *Staphylococcus aureus* and *Enterococci*. Cold Spring Harb. Perspect. Med. *6*, a026997.

Mogi, T., Murase, Y., Mori, M., Shiomi, K., Omura, S., Paranagama, M.P., and Kita, K. (2009). Polymyxin B identified as an inhibitor of alternative NADH dehydrogenase and malate: quinone oxidoreductase from the gram-positive bacterium *Mycobacterium smegmatis*. J. Biochem. *146*, 491–499.

Peng, B., Su, Y.B., Li, H., Han, Y., Guo, C., Tian, Y.M., and Peng, X.X. (2015). Exogenous alanine and/or glucose plus kanamycin kills antibiotic-resistant bacteria. Cell Metab. *21*, 249–262.

Rao, S.P.S., Alonso, S., Rand, L., Dick, T., and Pethe, K. (2008). The proton motive force is required for maintaining ATP homeostasis and viability of hypoxic, nonreplicating *Mycobacterium tuberculosis*. Proc. Natl. Acad. Sci. U S A *105*, 11945–11950.

Sonenshein, A.L. (2007). Control of key metabolic intersections in *Bacillus subtilis*. Nat. Rev. Microbiol. *5*, 917–927.

Straus, S.K., and Hancock, R.E. (2006). Mode of action of the new antibiotic for Gram-positive pathogens daptomycin: comparison with cationic antimicrobial peptides and lipopeptides. Biochim. Biophys. Acta *1758*, 1215–1223.

Su, Y.B., Peng, B., Li, H., Cheng, Z.X., Zhang, T.T., Zhu, J.X., Li, D., Li, M.Y., Ye, J.Z., Du, C.C., et al. (2018). Pyruvate cycle increases aminoglycoside efficacy and provides respiratory energy in bacteria. Proc. Natl. Acad. Sci. U S A *115*, E1578–E1587.

Trimble, M.J., Mlynarcik, P., Kolar, M., and Hancock, R.E. (2016). Polymyxin: alternative mechanisms of action and resistance. Cold Spring Harb Perspect. Med. *6*, a025288.

Wosten, M.M.S.M., Kox, L.F.F., Chamnongpol, S., Soncini, F.C., and Groisman, E.A. (2000). A signal transduction system that responds to extracellular iron. Cell *103*, 113–125.

Xing, Y.H., Wang, W., Dai, S.Q., Liu, T.Y., Tan, J.J., Qu, G.L., Li, Y.X., Ling, Y., Liu, G., Fu, X.Q., et al. (2014). Daptomycin exerts rapid bactericidal activity against *Bacillus anthracis* without disrupting membrane integrity. Acta Pharmacol. Sin. *35*, 211–218.

Yang, J., Zeng, Z.H., Yang, M.J., Cheng, Z.X., Peng, X.X., and Li, H. (2018). NaCl promotes antibiotic resistance by reducing redox states in *Vibrio alginolyticus*. Environ. Microbiol. *20*, 4022–4036.

Yu, W.B., Yin, C.Y., Zhou, Y., and Ye, B.C. (2012). Prediction of the mechanism of action of fusaricidin on *Bacillus subtilis*. PLoS One *7*, e50003.

ISCI, Volume *21*

Supplemental Information

Glucose-Induced Cyclic Lipopeptides Resistance in Bacteria via ATP Maintenance through Enhanced Glycolysis

Wen-Bang Yu, Qian Pan, and Bang-Ce Ye

Supplemental Figures

Figure S1. Numbers of differentially expressing proteins (P-value < 0.05) in treatments of glucose, PB plus glucose and glucose, respectively. Related to Figure 2.

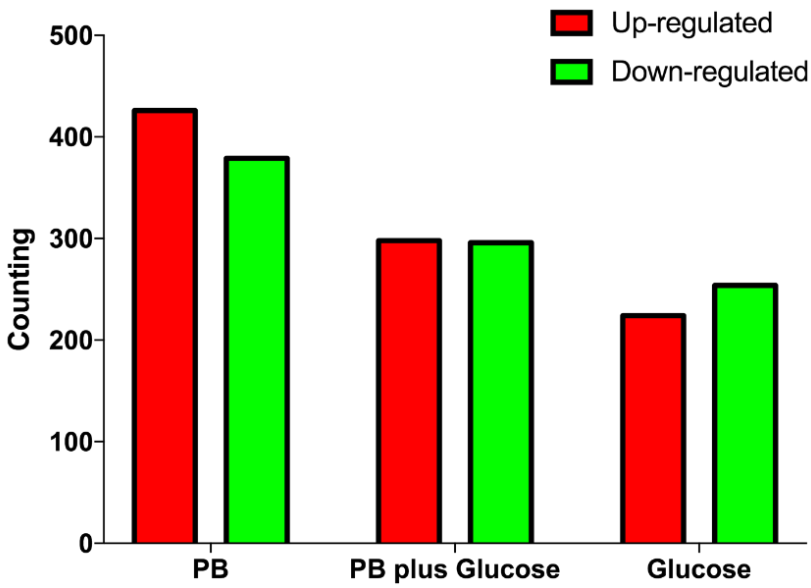

Expression of 805 (379 proteins were down-regulated and 426 proteins were up-regulated), 594 (296 proteins were down-regulated and 298 proteins were up-regulated), and 478 (254 proteins were down-regulated and 224 proteins were up-rregulated) proteins were found to be significantly changed after treatment by PB, PB plus glucose, or glucose, respectively.

Transparent Methods

Bacterial strains, materials, and growth conditions

Bacillus subtilis ATCC21616, *Staphylococcus aureus* ATCC12600 were firstly grown in glass flasks with the Luria-Bertani (LB) medium at 37 °C and 220 rpm. When the OD_{600} of culture reach 0.3, the culture was split into 50 ml centrifuge tubes for adding polymyxin B (50 μg/ml), daptomycin (5 μg/ml), vancomycin (50 μg/ml), glucose (5-20 mM), fructose (20 mM), arabinose (20 mM), glycerol (20 mM), inhibitor et al. The final volume in each tube is 3ml. The same amount of bacteria culture was collected for ATP and metabolite detection. All carbon source, inhibitor and PB were purchased from Sigma Aldrich (St. Louis, MO, USA). Antibiotics were filtered with a 0.22 mm pore size hydrophilic PVDF membrane. Luria-Bertani (LB) were sterilized by autoclaving at 121 °C for 20 min. *Bacillus subtilis* ATCC21616 were grown to reach 1.0 of OD value for cell membrane preparation.

Screening of carbon source

Bacillus subtilis ATCC21616, *Staphylococcus aureus* ATCC12600 were firstly grown in glass flasks with the Luria-Bertani (LB) medium at 37 °C and 220 rpm. When the OD_{600} of culture reach 0.3, the culture was split into 50 ml centrifuge tubes for adding polymyxin B (50 μg/ml), daptomycin (5 μg/ml), vancomycin (50 μg/ml), glucose (5-20 mM), fructose (20 mM), arabinose (20 mM), glycerol (20 mM), inhibitor et al. The final volume in each tube is 3ml. The same amount of bacteria culture was collected for ATP and metabolite detection. All carbon source, inhibitor and PB were purchased from Sigma Aldrich (St. Louis, MO, USA). Antibiotics were filtered with a 0.22 mm pore size hydrophilic PVDF membrane. Luria-Bertani (LB) were sterilized by autoclaving at 121 °C for 20 min. *Bacillus subtilis* ATCC21616 were grown to reach 1.0 of OD value for cell membrane preparation.

Preparation of *Bacillus subtilis* membranes

After reaching an OD_{600} of 1.0, *Bacillus subtilis* ATCC21616 cells were collected using centrifugation at 3,500 r.p.m. for 30 min at 4 °C and washed twice using buffer solution containing 30 mM Tris–HCl and 10 mM Na-EDTA (pH 7.5). Cells were resuspended with 30 mM Tris–HCl, 10 mM Na-EDTA (pH 7.5), and protease inhibitor cocktail. The strains were lysed using high pressure at 13–14 MPa and centrifuged at 12,000 g for 15 min at 4 °C. Membranes were recovered from the supernatant using centrifugation at 150,000 g for 60 min at 4 °C and resuspended with 30 mM Tris–HCl (pH 7.5).

Detection of NADH dehydrogenase activities

NADH dehydrogenase activity assays were started using 10 mg/ml membranes, 200 mM NADH, 100 mM Q1, 50 mM Tris–HCl (pH 7.5), and 0.05% Tween 20. In the real-time monitoring of the enzymatic reaction, measurements of absorbance at 340 nm were acquired every 30 s for 10 min. For inhibition studies, the reaction mixture was

preincubated with polymyxin B (0, 20, 30, 40, 50, 75, 100 μg/ml) for 10 min. The decreased values of absorbance were simulated using GraphPad Prism 5 (GraphPad Software, Inc., La Jolla, CA) to get the 50% inhibitory concentration (IC50) of polymyxin B.

ATP level determination

ATP detection kit was purchased from Beyotime Biotechnology (Shanghai, China). The kit is based on firefly luciferase which uses ATP to catalyze luciferin to produce fluorescence. When firefly luciferase and luciferin are both in excess, fluorescent production is proportional to the concentration of ATP. The same amounts of bacteria (10^8 cells) were lysed in ice water mixture for 15 min by ATP detection lysis buffer to release ATP. The fluorescence value was measured using the microplate reader SynergyTM Mx (Bio-Tek Instruments, Winooski, VT) after adding ATP detection reagent.

Determination of glucose and organic acid levels

The glucose detection kit was purchased from Sigma Aldrich (St. Louis, MO, USA). First, ATP phosphorylates glucose via hexokinase. In the presence of oxidation type nicotinamide adenine dinucleotide (NAD^+), glucose-6-phosphate was phosphorylated to produce 6-phosphoric acid-gluconic acid by glucose-6-phosphate dehydrogenase (G6PDH). In the oxidation reaction, the increased absorption value of 340 nm is directly proportional to the glucose concentration. The same amounts of bacteria (10^8 cells) were lysed in ice water mixture for 15 min by glucose detection lysis buffer to release glucose. The absorption value was measured using the microplate reader SynergyTM Mx (Bio-Tek Instruments, Winooski, VT) after adding the glucose assay reagent.

For determination of organic acids (pyruvate and acetate), 10^9 cells were collected. Metabolites from the cell pellets were extracted with 200 μl 5% $HClO_4$ in an ice bath for 15 min. After centrifugation at 10000 g for 5 min, the supernatant was neutralized with a K_2CO_3 solution, and the $KClO_4$ precipitate was removed by centrifugation. Subsequently, the levels of organic acids were determined by High Performance Liquid Chromatography. HPLC condition was 0.013 M H_2SO_4 at a flow rate of 1.0 mL/min and 40 °C. UV spectra were acquired at 210 nm.

Proteomic analysis

The aim of this project was to use an integrated approach involving TMT labeling and LC-MS/MS to quantify the dynamic changes of the whole proteome of *B. subtilis*. The general work flow is indicated as follows: protein extraction, trypsin digestion, TMT labeling, HPLC fractionation, LC-MS/MS analysis, database search, and bioinformatics analysis.

Sample was first grinded by liquid nitrogen, then the cell powder was transferred to 5

mL centrifuge tube and sonicated three times on ice using a high intensity ultrasonic processor (Scientz) in lysis buffer (8 M urea, 2 mM EDTA, 10 mM DTT, and 1% Protease Inhibitor Cocktail III). The remaining debris was removed by centrifugation at 20,000 g at 4 °C for 10 min. Finally, the protein was precipitated with cold 15% TCA for 2 h at −20 °C. After centrifugation at 4 °C for 10 min, the supernatant was discarded. The remaining precipitate was washed with cold acetone three times. The protein was re-dissolved in buffer (8 M urea, 100 mM TEAB, pH 8.0) and the protein concentration was determined with 2-D Quant kit according to the manufacturer's instructions. After trypsin digestion, peptides were desalted using the Strata X C18 SPE column (Phenomenex) and vacuum-dried. Peptides were reconstituted in 0.5 M TEAB and processed according to the manufacturer's protocol for 6-plex TMT kit.

The sample was fractionated using high pH reverse-phase HPLC using Agilent 300Extend C18 column (5 μm particles, 4.6 mm ID, 250 mm length). Briefly, peptides were separated with a gradient of 2% to 60% acetonitrile in 10 mM ammonium bicarbonate pH 10 over 80 min into 80 fractions. The peptides were combined into 18 fractions and dried by vacuum centrifuging.

Peptides were dissolved in 0.1% FA, directly loaded onto a reversed-phase pre-column (Acclaim PepMap 100, Thermo Scientific). Peptide separation was performed using a reversed-phase analytical column (Acclaim PepMap RSLC, Thermo Scientific). The gradient was comprised of an increase from 6% to 22% solvent B (0.1% FA in 98% ACN) over 26 min, 22% to 35% in 8 min and climbing to 80% in 3 min then holding at 80% for the last 3 min, all at a constant flow rate of 350 nl/min on an EASY-nLC 1000 UPLC system. The resulting peptides were analyzed by Q ExactiveTM plus hybrid quadrupole-Orbitrap mass spectrometer (ThermoFisher Scientific).

The peptides were subjected to NSI source followed by tandem mass spectrometry (MS/MS) in Q ExactiveTM plus (Thermo) coupled online to the UPLC. Intact peptides were detected in the Orbitrap at a resolution of 70,000. Peptides were selected for MS/MS using an NCE setting of 30. Ion fragments were detected in the Orbitrap at a resolution of 17,500. A data-dependent procedure that alternated between one MS scan followed by 20 MS/MS scans was applied for the top 20 precursor ions above a threshold ion count of 10000 in the MS survey scan with 30.0s dynamic exclusion. The electrospray voltage applied was 2.0 kV. Automatic gain control (AGC) was used to prevent overfilling of the orbitrap; 5E4 ions were accumulated for generation of MS/MS spectra. For MS scans, the m/z scan range was 350 to 1800. Fixed first mass was set as 100 m/z.

The resulting MS/MS data were processed using Mascot search engine (v.2.3.0). Tandem mass spectra were searched against Uniprot *Bacillus Subtilis* (strain 168) database. Trypsin/P was specified as cleavage enzyme allowing up to 2 missing cleavages. Mass error was set to 10 ppm for precursor ions and 0.02 Da for fragmentations. Carbamidomethyl on Cys were specified as fixed modifications, and

oxidation on Met was specified as variable modifications. For protein quantification method, TMT-6-plex was selected in Mascot. FDR was adjusted to < 1% and peptide ion score was set ≥ 20.